Neuro-Oncology Advances
3(1), 1–11, 2021 | doi:10.1093/noajnl/vdaa165 | Advance Access date 3 December 2020

A brain-penetrant microtubule-targeting agent that disrupts hallmarks of glioma tumorigenesis

Eric A. Horne, Philippe Diaz, Patrick J. Cimino, Erik Jung, Cong Xu, Ernest Hamel, Michael Wagenbach, Debra Kumasaka, Nicholas B. Wageling, Daniel D. Azorín, Frank Winkler, Linda G. Wordeman, Eric C. Holland, and Nephi Stella

Department of Pharmacology, University of Washington, Seattle, Washington, USA (E.A.H., C.X., N.S.); Stella Therapeutics, Inc., Pacific Northwest Research Institute, Seattle, Washington, USA (E.A.H.); Department of Biomedical and Pharmaceutical Sciences, University of Montana, Missoula, Montana, USA (P.D.); DermaXon LLC, Missoula, Montana, USA (P.D., N.B.W.); Department of Pathology, University of Washington, Seattle, Washington, USA (P.J.C.); Neurology Clinic and National Center for Tumor Diseases, University Hospital Heidelberg, Heidelberg, Germany (E.J., D.D.A., F.W.); Developmental Therapeutics Program, Frederick National Laboratory for Cancer Research, Frederick, Maryland, USA (E.H.); Department of Physiology and Biophysics, University of Washington, Seattle, Washington, USA (M.W., L.G.W.); Division of Human Biology, Fred Hutchinson Cancer Research Center, Seattle, Washington, USA (D.K., E.C.H.); Department of Psychiatry and Behavioral Sciences, University of Washington, Seattle, Washington, USA (N.S.)

Corresponding Author: Nephi Stella, PhD, Department of Psychiatry and Behavioral Sciences, University of Washington, 1959 NE Pacific Street, Seattle, WA 98195-5280, USA (nstella@uw.edu).

Abstract

Background. Glioma is sensitive to microtubule-targeting agents (MTAs), but most MTAs do not cross the blood brain barrier (BBB). To address this limitation, we developed the new chemical entity, ST-401, a brain-penetrant MTA.

Methods. Synthesis of ST-401. Measures of MT assembly and dynamics. Cell proliferation and viability of patient-derived (PD) glioma in culture. Measure of tumor microtube (TM) parameters using immunofluorescence analysis and machine learning-based workflow. Pharmacokinetics (PK) and experimental toxicity in mice. In vivo antitumor activity in the RCAS/tv-a PDGFB-driven glioma (PDGFB-glioma) mouse model.

Results. We discovered that ST-401 disrupts microtubule (MT) function through gentle and reverisible reduction in MT assembly that triggers mitotic delay and cell death in interphase. ST-401 inhibits the formation of TMs, MT-rich structures that connect glioma to a network that promotes resistance to DNA damage. PK analysis of ST-401 in mice shows brain penetration reaching antitumor concentrations, and in vivo testing of ST-401 in a xenograft flank tumor mouse model demonstrates significant antitumor activity and no over toxicity in mice. In the PDGFB-glioma mouse model, ST-401 enhances the therapeutic efficacies of temozolomide (TMZ) and radiation therapy (RT).

Conclusion. Our study identifies hallmarks of glioma tumorigenesis that are sensitive to MTAs and reports ST-401 as a promising chemical scaffold to develop brain-penetrant MTAs.

Key Points

- The microtubule-targeting agent, ST-401, crosses the blood brain barrier and reaches antitumor concentrations in brain.
- ST-401 disrupts glioma tumorigenesis by triggering mitotic delay and cell death in interphase, disrupting tumor microtubes and enhancing the therapeutic efficacies of standard care treatments.

Importance of the Study

Most cancer therapeutics to not cross the BBB and are therefore ineffective in treating glioma. We report the developed a brain-penetrant MTA, ST-401, and found that it disrupts multiple hallmarks of glioma tumorigenesis, including the formation of TMs that convey resistance to standard of care treatments. In a preclinical mouse model of glioma, ST-401 enhances the efficacy of standard of care treatments. Brain-penetrant MTAs hold breakthrough potential as they harbor preclinical characteristics that promise therapeutic benefit for the treatment of glioma.

Microtubule-targeting agents (MTAs) act by binding to either tubulin dimers or assembled microtubule (MT). Depending on their mechanism of action (MOA), they disrupt MT assembly, disassembly and dynamics, all of which alter fundamental cell functions such as mitosis, cell migration, vesicle transport and intracellular signaling.[1,2] MTAs trigger cell death by multiple mechanisms, including prolonged activation of the spindle assembly checkpoint (SAC) during mitosis and by inducing senescence in interphase.[3] Multiple lines of evidence suggest that glioma is particularly sensitive to MTAs; however most MTAs do not cross the blood–brain barrier (BBB) and have limited therapeutic value in neuro-oncology.[4]

Three hallmarks of glioma tumorigenesis are sensitive to MTAs. First, this cancer often carries mutations that result in altering MT dynamics and increase baseline chromosome instability that contributes to tumorigenesis, rendering glioma particularly sensitive to the MT disrupting effect of MTA.[5] Second, glioma treated with MTAs dies through SAC arrest.[6] Third, glioma tumorigenesis is facilitated by intercellular connections, tumor microtubes (TMs), that link malignant cells in a syncytium that promotes resistance to standard care therapies by transfer of cellular factors and organelles involved in homeostasis and self-repair.[7–9] Furthermore, TMs are prerequisite neurite-like protrusions that enable diffuse infiltration of glioma in brain parenchyma that is behind an intact BBB.[10] SinceTMs are characterized by a high content of MTs that appear to mediate rapid intra-TM transport of factors and organelles, it is possible that brain-penetrant MTAs could be highly effective at curbing glioma tumorigenesis by disrupting this cellular syncytium.[10] Brain-penetrant MTAs have been recently developed, and patients treated thus far have shown good tolerability in a small Phase I/II study.[11] Combined, these evidence suggest that glioma can be particularly sensitive to alterations in MT function and highlights the need to develop brain-penetrant MTAs to treat this devastating disease.

There are 6 ligand-binding sites on tubulin that disrupt MT function through distinct MOAs: two sites targeted by microtubule-stabilizing agents (the taxane and the laulimalide/peloruside sites) and four sites targeted by microtubule-destabilizing agents (MDA) (the colchicine, the vinca, the maytansine, and the pironetin sites).[12] In previous studies, we developed MDAs (ST-34, ST-360, and ST-377) that bind to the colchicine site of tubulin, inhibit MT assembly, and kill glioma cells in culture (ie, compounds 8, 20, and 27 in ref. [13]; Figure 1A). Here we leveraged these results as the starting point to develop a novel chemical entity, ST-401, and studied its MOA and antitumor activity in glioma cells in culture and in the RCAS/tv-a PDGFB-driven glioma mouse model.

Methods

Animal Studies

Animal studies followed the guidelines established by AAALAC, and were approved by IACUC of the University of Washington, the Fred Hutchinson Cancer Research Center and the Pacific Northwest Research Institute.

Experimental Toxicity Studies

CD1 mice received 5, 10, 20, 50, 100, or 150 mg/kg ST-401 i.p., or the corresponding volume of no-drug formulation (vehicle). Mice were monitored for signs of general distress, as described.[14] Specifics are in Supplementary Methods.

Cells in Culture, Xenograft, and RCAS/tv-a PDGFB Glioma Mouse Models

Cells in culture, Xenograft and RCAS/tv-a PDGFB glioma mouse models were established as described.[14,15] Specifics are in Supplementary Methods.

[3H]Colchicine Binding to Tubulin, Tubulin Assembly, Cell Proliferation and Viability, Time-Lapse Microscopy, and Fluorescence Immunocytochemistry

[3H]Colchicine binding to tubulin, tubulin assembly, cell proliferation and viability, time-lapse microscopy, and fluorescence immunocytochemistry were performed as described.[14] Specifics are in Supplementary Methods.

Live Cell Imaging of MT Polymerization

HCT116 cells expressing EB1-GFP to label assembling MTs were imaged at a single Z-plane at 500-ms intervals

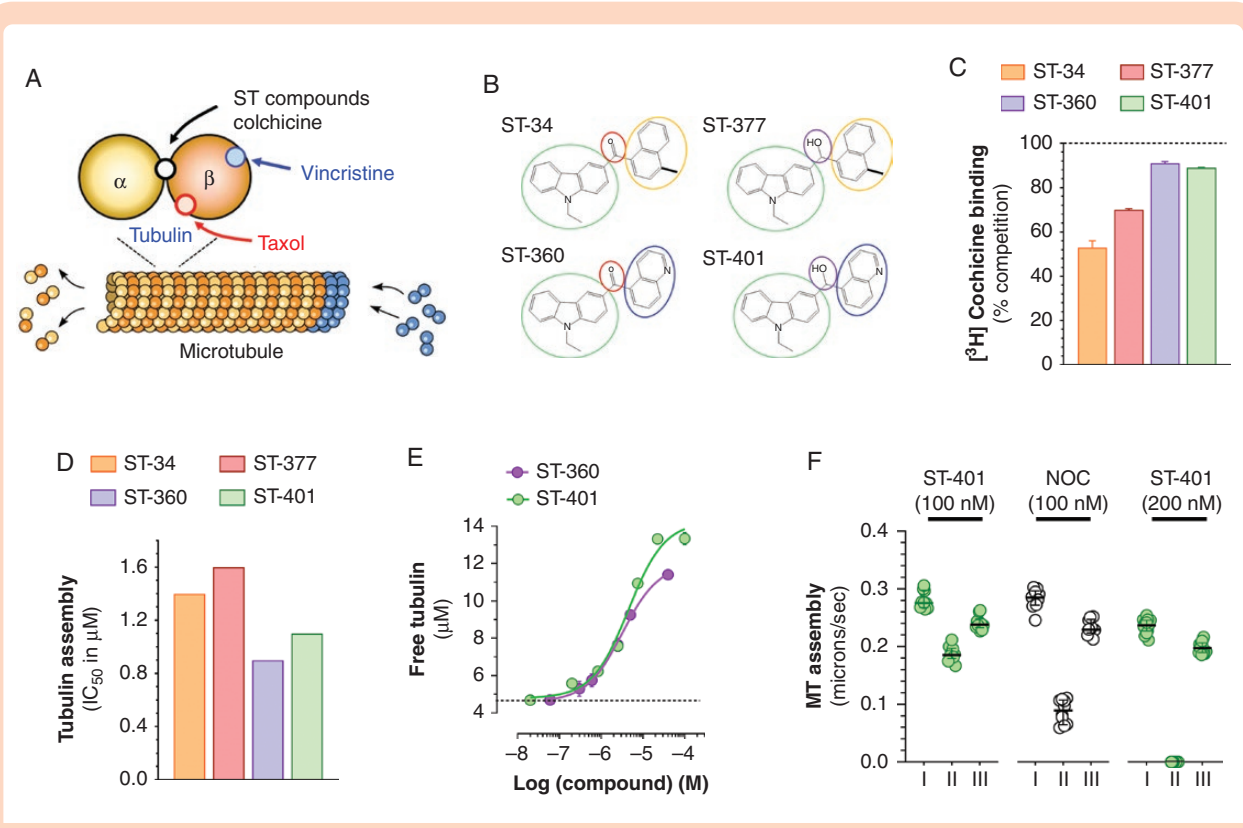

Figure 1. Activity of ST-401 and its analogues at the colchicine site of tubulin, and MT assembly and dynamics. (A) Diagram of MTA binding sites on tubulin. (B) ST-401 and its analogues are based on an *N*-ethyl-carbazole moiety (green) linked via a ketone (ST-34, ST-360, red) or a secondary alcohol (ST-377, ST-401, purple) to either a quinoline (ST-360, ST-401, blue) or a methyl-naphthalene residue (ST-34, ST-377, orange). (C) ST-compounds (5 μM) compete for [^{3}H]colchicine-binding to tubulin. Results are mean ± SD from $n = 3$ experiments. Dotted line shows vehicle control (5% DMSO). (D) ST-compounds inhibit tubulin assembly measured by turbidity development of tubulin solutions. Representative IC_{50} values from 3 experiments with comparable results. (E) ST-401 and ST-360 inhibit tubulin assembly measured in a pelleting assay. Results are mean ± SEM from 3 to 5 experiments. (F) ST-401 and nocodazole (NOC) reversibly inhibit MT assembly rates in HCT116 cells when comparing measures before (I), during (II), and after (III) treatment. $N = 10$–15 individual cells.

at on a Deltavision microscope system (Applied Precision, Issaquah, WA). MT assembly rates were scored in interphase cells using Fiji TrackMatec.[16] Specifics are in Supplementary Methods.

TMs Analysis

GFP-expressing, patient-derived S24 and BG5 cells were cultured, treated and analyzed as described.[7,17] Specifics are in Supplementary Methods.

Histological Analysis

Tumors were processed into formalin-fixed paraffin-embedded tissue blocks and slides as described.[18] Hematoxylin and eosin (H&E)-stained sections were blindly reviewed and scored by a board-certified neuropathologist (PJC). Automated immunohistochemical staining processing (Discovery, Ventana Medical Systems, Inc.). For semi-quantitative IHC analysis, tissue sections were analyzed using ImageJ. Specifics are in Supplementary Methods.

Statistical analysis

For comparisons between two groups of independent datasets, multiple *t* tests were performed, *P* value, mean and standard error of the mean (SEM) were reported. For comparisons among more than two groups (>2), one-way or two-way ANOVA were performed, *P* values and SEM were reported; and *P* values were adjusted by multiple testing corrections (Tuckey's post-test) when applicable.

Results

ST-401, a MTA That Reversibly Reduces MT Assembly

We developed ST-401 based on ST-34, ST-360, and ST-377 that kill glioma cells in culture with IC_{50} values of 268–630 nM.[13] ST-401 is a hybrid molecule that combines a secondary alcohol and quinoline in one structure (Figure 1B). Its chemical synthesis and analytical data are in Supplementary Figure S1. ST-401 competed for 89% of [^{3}H]colchicine binding to tubulin, which was comparable

to ST-360 (89%) and greater than ST-377 (70%) and ST-34 (53%) responses (Figure 1C).[13] In a turbidity assay, ST-401 inhibited tubulin assembly with an IC_{50} of 1.1 μM, a response comparable to the ST-360 response (IC_{50} = 0.9 μM), and more potent than the ST-377 and ST-34 responses (IC_{50}s = 1.4 and 1.6 μM, respectively) (Figure 1D). In a pelleting assay that measures release of free tubulin, ST-401 and ST-360 inhibited tubulin assembly with comparable IC_{50} values (3.2 and 4.5 μM, respectively),[14] but ST-401 triggered greater MT disassembly (ie, Δ release of free tubulin) compared to ST-360 (Figure 1E). These results show that ST-401 and ST-360 exhibit comparable binding and pharmacodynamic properties at the colchicine site of tubulin and yet ST-401 triggers more pronounced MT disassembly than ST-360.

To study the effect of ST-401 on MT assembly in cells, we used live cell imaging to track EB1-GFP on assembling MT ends in HCT116 cells in interphase, a model system that has been extensively characterized and serves as a reference with regard to real-time MT dynamics in cells in culture.[19] Specifically, we used EB1-GFP CRISPR HCT116 cells that express the EB1-GFP gene under its endogenous promotor to ensure that EB1-GFP expression does not influence baseline MT assembly rates and allow highly reproducible imaging quantification (Wordeman, unpublished). Here we compared MT assembly rates of cells treated with either ST-401 or nocodazole (NOC), a MDA that also binds to the colchicine site and exhibits a similar IC_{50} at inhibiting MT assembly relative to ST-401 as measured with biochemical assays (compare Figure 1E and Cherry et al.[14]). Figure 1F shows dots corresponding to mean MT assembly rates measured in individual HCT116 cells imaged at 3 times (before, during and after treatment). ST-401 (100 nM) triggered a milder reduction in MT assembly as compared to NOC (100 nM), even though these concentrations are equally effective at inhibiting MT assembly in biochemical assays. Another difference was that MTs were still visibly intact in HCT116 cells treated with 100 nM ST-401 (data not shown). This milder response of MTs to ST-401 contrasts with the well-known pronounced loss of tubulin polymer triggered by NOC.[20] Similar to NOC, the ST-401 response was reversible, as indicated by MT assembly reaching their initial rates within 15 min after wash-out (see POST, Figure 1F). Figure 1F also shows that ST-401 (200 nM) completely and reversibly inhibited all MT assembly within 15 min. Together, these results reveal a milder but similarly rapid onset and fully reversible MT dynamics response triggered by ST-401, together suggesting a promising safety feature for this new MTA.[21]

ST-401 Inhibits Multiple Hallmarks of Glioma Tumorigenesis

We subjected ST-401 to the NCI-60 cell line panel screening platform that includes six human glioma cell lines, and compared its response to the response of ST-34, ST-360, and ST-377.[13] ST-401 and ST-360 exhibited similar antitumor activities in the low nanomolar range in most human cancer cell lines (data not shown), including the six glioma lines (SF-268, SF-295, SF-539, SNB-19, SNB-75, and U251: IC_{50}s 23–69 nM) (Figure 2A). ST-34 and ST-377 activities were approximately 10-fold less potent in these cancer cell lines (IC_{50}s ranged from 239 to 877 nM) (Figure 2A). Thus, ST-401 possesses similar antitumor activity as ST-360 in human cancer cell lines in culture.

Glioma cell lines do not phenocopy the molecular heterogeneity of human glioma that led to their categorization in subtypes, including proneural (PN), mesenchymal (MES), and classical (CL) transcriptional subtypes.[22] We tested the antitumor activity of ST-401 in 3 PD-glioma isolates in culture (one of each subtype as in our previous study[13]), as well as in MGG8 cells, PD-glioma isolates that exhibit cancer stem cell properties.[23] Signficantly, the antitumor activity of ST-401 in PD-glioma was in the low nanomolar (IC_{50}: 24–47 nM), whereas ST-34, ST-377, and ST-360 were all less active (IC_{50}: 316–598 nM) (Figure 2B). These results showed that ST-401 exhibits enhanced antitumor activity in the low nanomolar range in PD-glioma irrespective of their subtype.

To better understand the antitumor activity of ST-401 in PD-glioma, we measured two endpoints in MGG8 cells treated for 72 h: the overall cell viability using the mitochondrial probe, WST-1, and the number of cells that entered S phase using Brd-U incorporation. The human glioma cell line, T98G, was used for comparison as it has a similar rate of cell proliferation (Supplementary Figure S2) and is sensitive to ST-compounds.[13] ST-401 reduced overall cell viability in MGG8 and T98G cells with comparable IC_{50}s (14 and 36 nM, respectively) (Figure 2C). NOC (3 μM) reduced MGG8 cell viability by 18% without affecting T98G cell viability (Figure 2D). MPS-1 IN, a check point kinase monopolar spindle 1 inhibitor involved in SAC initiation,[24] reduced MGG8 and T98G cell viability by 19 and 24%, respectively (Figure 2D). Thus, when measuring overall cell viability, MTAs exhibit similar activities in human glioma cell lines and PD-glioma. Remarkably, ST-401 reduced the number of MGG8 cells in S phase and this response was absent in T98G cells (Figure 2E). While MPS-1 IN also reduced the number of MGG8 cells in S phase, and was inactive in T98G cells, NOC (3 μM) was overall less active (Figure 2F) These results suggest that PD-glioma in interphase exhibit enhanced sensitivity to the disruption of MT function.

To test if ST-401 inhibits TM activity, we selected S24 and BG5 PD-glioma isolates that extend TMs and expresses GFP to visualize TMs by fluorescence microscopy. Two TM parameters were measured (TM number per cell and TM length per cell) in a semi-automatic manner using immunofluorescence images and machine learning-based workflow.[25] As expected, Y-27632, an inhibitor of the actomyosin cytoskeleton regulator p160ROCK, increased the number and length of TM in S24 and BG5 cells (Figure 3A–D). Y-27632 did not affect cell viability over this short time period (Supplementary Figure S3). Noco (300 nM) decreased both the number and length of TMs in S24 and only the number of TMs in BG5 cells (Figure 3C–E). TMs in S24 were more sensitive to increasing concentrations of ST-401 as indicated by more pronounced reductions in both the length and number of TMs in S24 cells compared to BG5 cells (Figure 3F–I). These results showed that ST-401 and Noco differentially decrease TM number in PD-glioma and that their ability to reduce TM length varies depending on the PD-glioma (here S24 is more sensitive

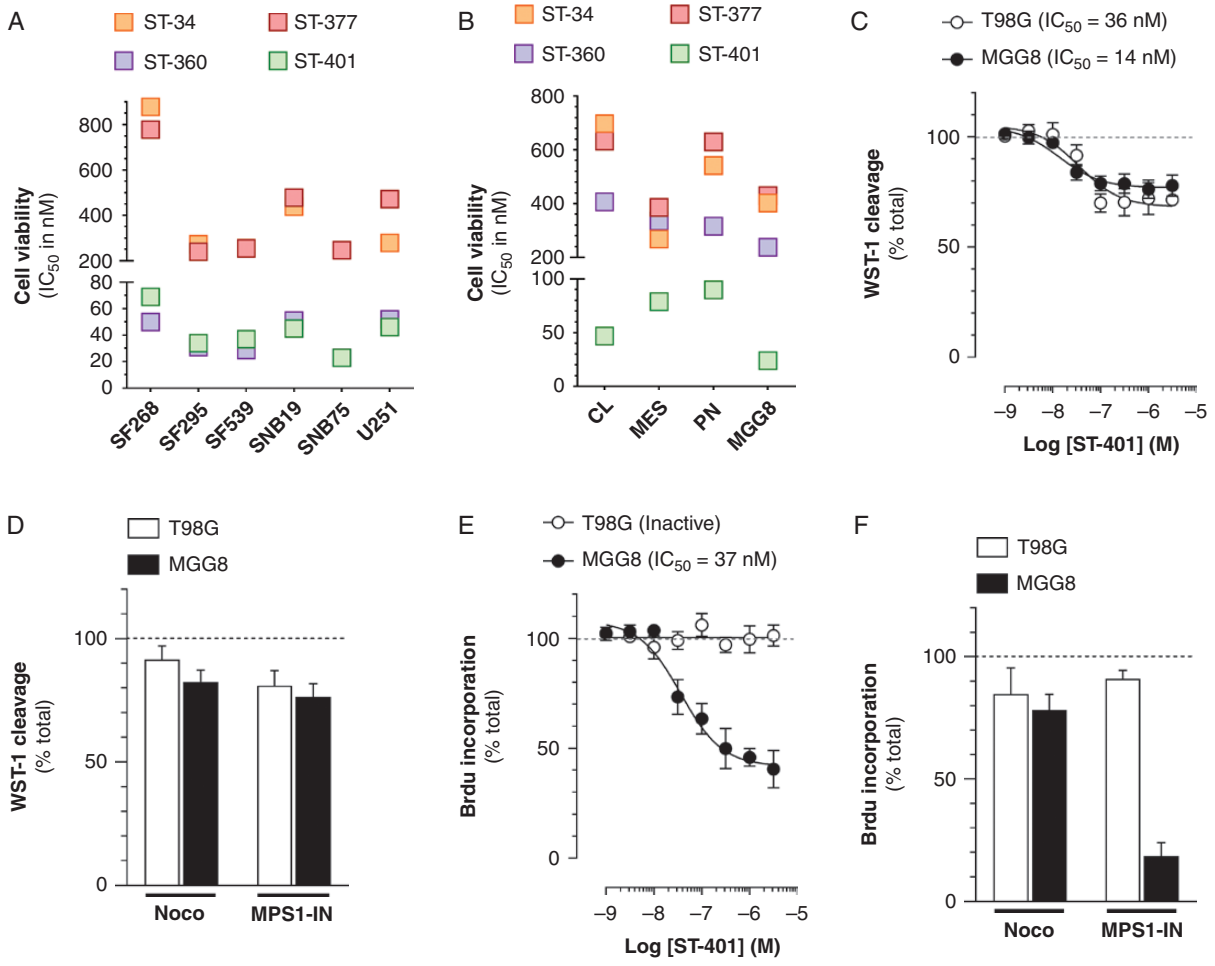

Figure 2. Broader antitumor activity of ST-401 in PD-glioma compared to glioma cell lines in culture. (A) ST-compounds inhibit the growth (TGI_{50}) of 6 human glioma cell lines in the NCI-60 cell line panel. (B) ST-compounds reduce the viability of 4 PD-glioma isolates when measuring WST-1 cleavage. Results are mean ± SEM from 3 to 5 experiments. (C) ST-401 reduces the viability of T98G and MGG8 cells with comparable IC_{50}s when measuring WST-1 cleavage. (D) NOC (3 μM) and MPS1-IN (30 μM) reduce the viability of T98G and MGG8 cells when measuring WST-1 cleavage. (E) ST-401 reduces the number of MGG8 cell in S phase when measuring BrdU-incorporation. Lack of response in T98G. (F) NOC (3 μM) and MPS1-IN (30 μM) reduce the number of MGG8 cell in S phase when measuring BrdU-incorporation. Lack of response in T98G and cells. (C–F) Results are mean ± SEM from $n = 3$–6 experiments. Two-way ANOVA analysis followed by Tuckey's post-test indicated significance of $^{*}P < .05$, $^{**}P < .01$ and $^{***}P < .001$ compared to vehicle control (dotted line).

than BG5). Together, our results showed that ST-401 inhibits multiple traits of glioma tumorigenesis measured in cell culture model systems, which provided impetus to study its in vivo antitumor activity.

ST-401 Dose Range Finding, Pharmacokinetic Profile, and Antitumor Activity in a Xenograft Flank Model

We developed a stable formulation of ST-401 (Supplementary Figure S4), and found that the acute maximal tolerated dose (MTD) for single i.p. injections of ST-401 was 150 mg/kg. Dose range finding (DRF) study (one i.p. injection/day, 5 days/week for 4 weeks) showed that 20 mg/kg was tolerated as indicated by mice gaining weight normally and not showing signs of distress, as well as the lack of tissue lesions analyzed in 6 organs (Regimen 1) (Supplementary Figure S5A–D).

A limiting factor of most current MTAs is their inability to cross the BBB.[26] We injected mice with ST-401 at its acute MTD (150 mg/kg) and quantified the amounts of ST-401 reached in both plasma and brain by LC–MS (Supplementary Figure S6).[14] Figure 4A shows that ST-401 readily reached micromolar concentrations in mouse brain (ie, concentrations that are above its antitumor activity in culture) with a half-life of approximately 6 h and a brain/plasma ratio of 2.2 that indicated favorable brain penetration. Treatment with 20 and 5 mg/kg also resulted in micromolar concentrations in mouse brain (Figure 4B).

Considering these results, we tested if two injections per day of ST-401 at 20 mg/kg (total daily dose 40 mg) would

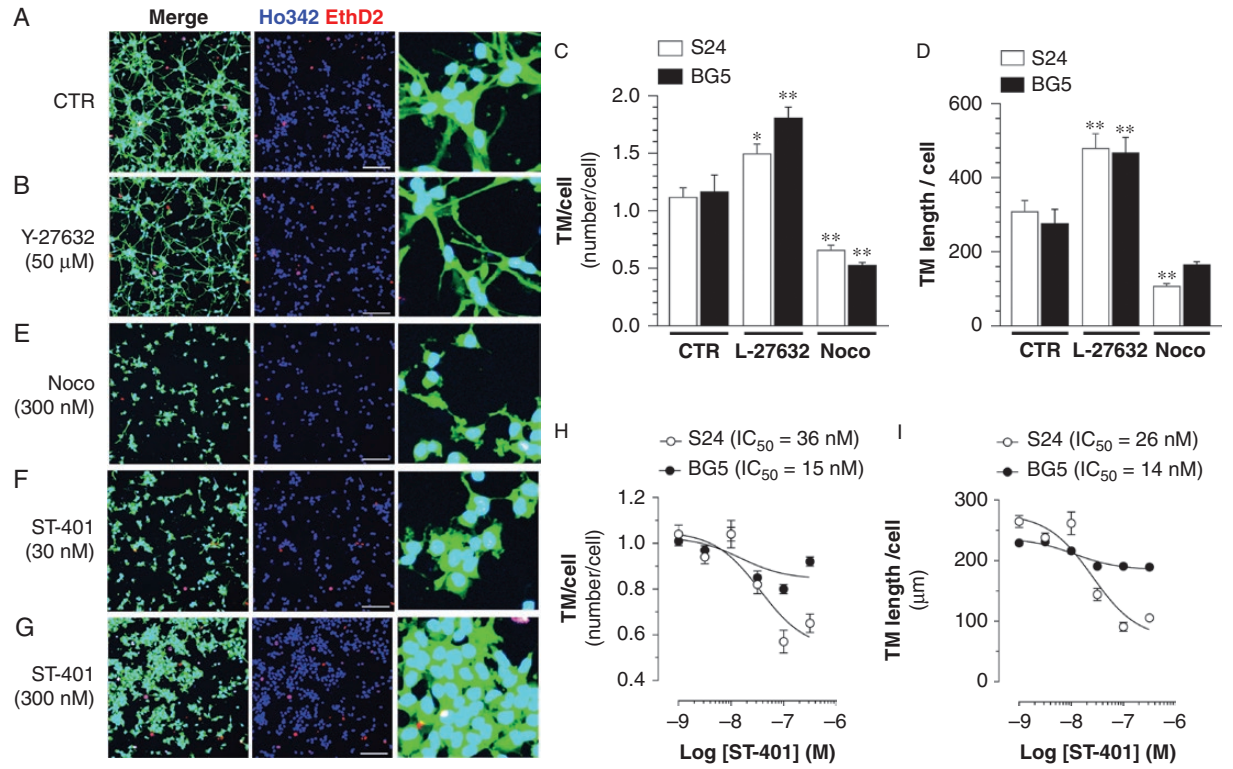

Figure 3. ST-401 decreases TM number and length in PD-glioma cells in culture. Representative images of PD glioma (S24) expressing cytoplasmatic GFP and treated with vehicle control (DMSO 1%) (A), Y-27632 (50 μM) (B), Noco (300 nM) (E) and ST-401 (30 and 300 nM) (F and G), and stained with Ho342 and EthD2 fluorescence. Scale bar = 200 μm. (C–D) Y-27632 (50 μM) increased, and Noco (300 nM) decreased, TM number/cell (C) and TM length/cell (D). (H–I) ST-401 decreased TM number/cell (H) and TM length/cell (I) in S24 PD-glioma to greater extent than in BG5 PD-glioma. Two-way ANOVA analysis followed by Tuckey's post-test indicated significance of $*P < .05$ and $***P < .001$ compared to vehicle control (DMSO 1%). Microtube length and number per cell were quantified in a semi-automatic manner using immunofluorescence images and machine learning-based workflow.

both be safe and increase the drug exposure time. The DRF study of bidaily injection of ST-401 (20 mg/kg, 5 days/week for 4 weeks) did not trigger adverse effects, mice gained weight normally and showed no signs of distress and tissue lesions (Regimen 2) (Supplementary Figure S5E–G). Bidaily injections of ST-401 at 20 mg/kg resulted in plasma blood levels that remained above 250 nM for approximately 16 h (Figure 4C).

As a first evaluation of the potential in vivo antitumor activity of ST-401, we selected the COLO205 xenograft mouse model because it reliably forms flank tumors that are commonly used as first test of the in vivo antitumor activity of novel therapeutics, and because COLO205 cells are sensitive to ST-401 (IC_{50} = 38 nM, data from the NCI-60 cancer cell panel). Figure 4D shows that COLO205 flank tumors in the vehicle control arm grew rapidly (by 400–550% in 20–30 days), resulting in all mice reaching end stage by 36 days (maximal tumor volume = 1500 mm^3). By contrast, tumors treated with ST-401 (Regimen 2) grew only half as fast (by 200–250% in 20–30 days). Note that approximately 50% of the treated tumors stopped growing despite ending the treatment and that these tumors did not recur before an additional 28 d (Figure 4D). Thus, the therapeutic response to ST-401 led to doubling of the life-expectancy of treated mice (Figure 4E). These results showed that treating mice with ST-401 using the regimen that we established (Regimen 2) might result in significant antitumor activity and provided a foundation to test the antitumor activity of ST-401 in an orthotopic and immunocompetent mouse model of glioma, as features of the native microenvironment, such as tumor–stroma interactions occurring behind the BBB, are critical modulators of tumorigenesis and response to standard care treatment.[27]

ST-401 Enhances the Therapeutic Efficacy of TMZ and RT in PDGFB-Glioma Mouse Model

The RCAS/tv-a PDGFB glioma mouse model harbors key features: it develops invasive high-grade glioma with histopathological features similar to human glioma in an incompetent host, and it responds to the TMZ and RT regimens used in human patients.[18] Thus, this model system provided a more meaningful insight in the antiglioma activity of ST-401 to tease apart if and when this drug might be useful to treat patients. Our experimental design included six treatment arms: (1) control, (2) TMZ (50 mg/kg, once per day, 5 days/week for 4 weeks) and (3) RT (upfront

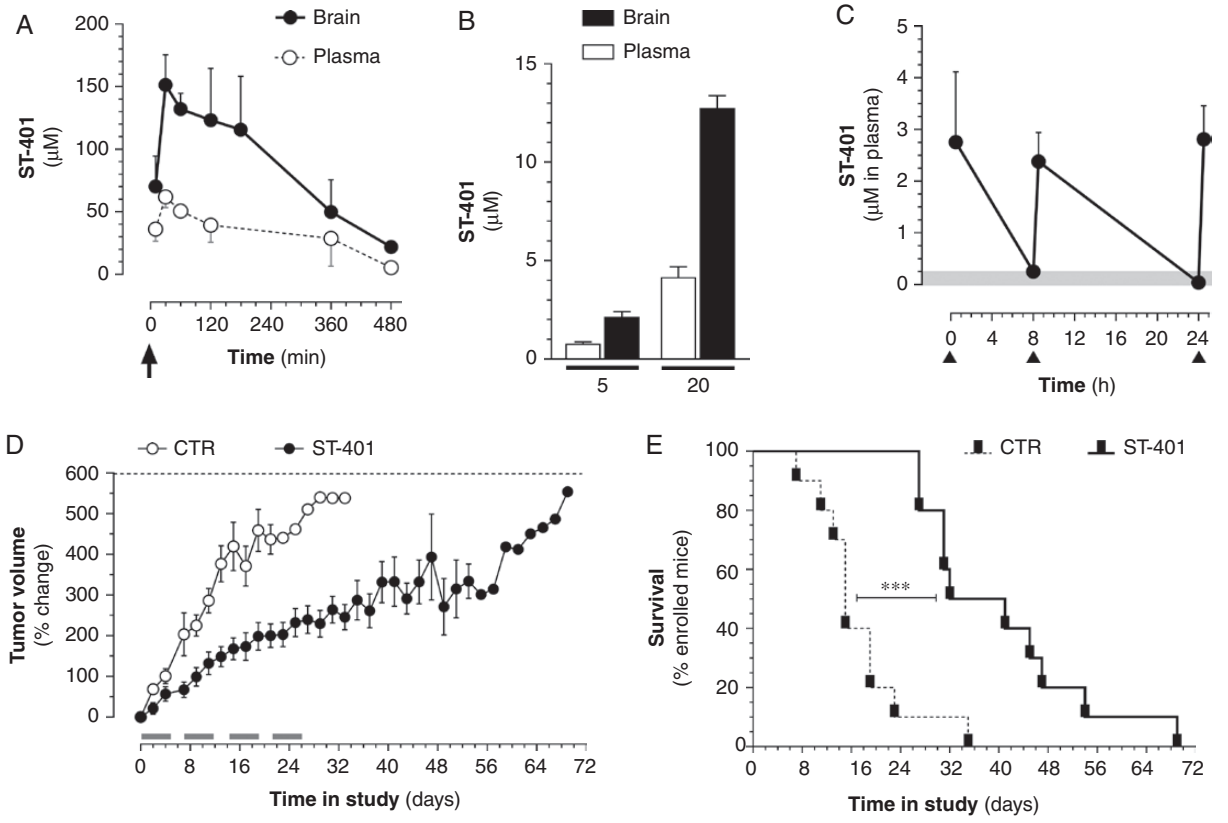

Figure 4. ST-401 penetrates mouse brain and exhibits antitumor activity in a xenograft flank tumor model. (A) Time course of ST-401 in mouse plasma and brain after a single i.p. injection of 150 mg/kg (arrow) showed that ST-401 readily penetrated the brain as measured by LC-MS. (B) ST-401 in mouse plasma and brain after a single i.p. injection of 5 mg/kg and 20 mg/kg showed that ST-401 reached micromolar concentrations in brain 30 min following treatment as measured by LC-MS. (C) Time course of ST-401 in mouse plasma resulting from three i.p. injections of ST-401 (20 mg/kg) separated by 8 and 16 h (arrows) showed that ST-401 remained above 250 nM (gray area) over 24 h. Results are mean ± SEM from $n = 5$ mice per time point. (D) Effect of bidaily injection of ST-401 (20 mg/kg, i.p.) on tumor volume of COLO205 cell -derived subcutaneous xenografts. Gray bars indicate ST-401 treatment days (5 d/wk for 4 wk). Dotted line indicates end-stage defined as tumor > 1500 mm^3. (E) Kaplan Meier survival curves shows significant increase in average survival (Log-rank (Mantel-Cox) test, Chi square 14.01, $P < .001$. Results are mean ± SEM of $n = 10$ mice per treatment arm.

single dose of 10-Gy), as previously described,[18,28] and (4) ST-401 (regimen 2), (5) ST-401 + TMZ, and (6) ST-401 + RT (Figure 5A). As expected, both RT and TMZ treatment extended the average median survival of glioma-baring mice by 90% and 50%, respectively (from 20 days to 38 days and 30 days, respectively) (Figure 5A). While ST-401 did not affect average median survival as single agent treatment, it enhanced the therapeutic efficacy of RT by 66%, and the therapeutic efficacy of TMZ by 60% (average survival in ST-401+RT arm = 50 days, and in ST-401+TMZ arm = 46 days) (Figure 5A). This result suggested that ST-401 acts as a radiosensiting agent that significantly enhances the therapeutic efficacy of DNA-damaging treatments. Histopathological analysis of PDGFB-glioma harvested at end-stage showed the expected increase in necrotic area in response to RT, and the unchanged necrotic area when treated with TMZ (Figure 5B–D). There was a trend toward ST-401 treatment to increase necrotic area and reduce the RT response on necrotic area that did not reach significance (Figure 5B). We also found no significant difference in apoptosis between treatment arms when quantifying cells expressing cleaved caspase-3 (Supplementary Figure S7).[29] One predicted outcome of ST-401 treatment was to disrupt glioma cell mitosis, and accordingly ST-401-treated PDGFB-glioma exhibited 69% more mitotic figures than the control arm, and most mitotic figures appeared disrupted (Figure 6A and B).[29] The genetic construct of PDGFB injected into mouse brains to generate glioma contains a hemagglutinin (HA) tag that facilitates the histological discrimination between oncogene-expressing tumor cells and nontumor stromal cells.[18] We performed a semi-quantitative IHC analysis of the relative area of HA expression in glioma as an index of tumor density and found that RT increased tumor density by 91% and ST-401 by 54% (Figure 6C–E and Figure S8). A similar increase in tumor density was measured when analyzing GBM tissue using Olig2 (a nuclear transcription factor) (Figure 6F–H and Figure S9). Increase in tumor density may reflect multiple cellular mechanisms, including stalling of round cancer cells in mitosis, shrinkage of dying

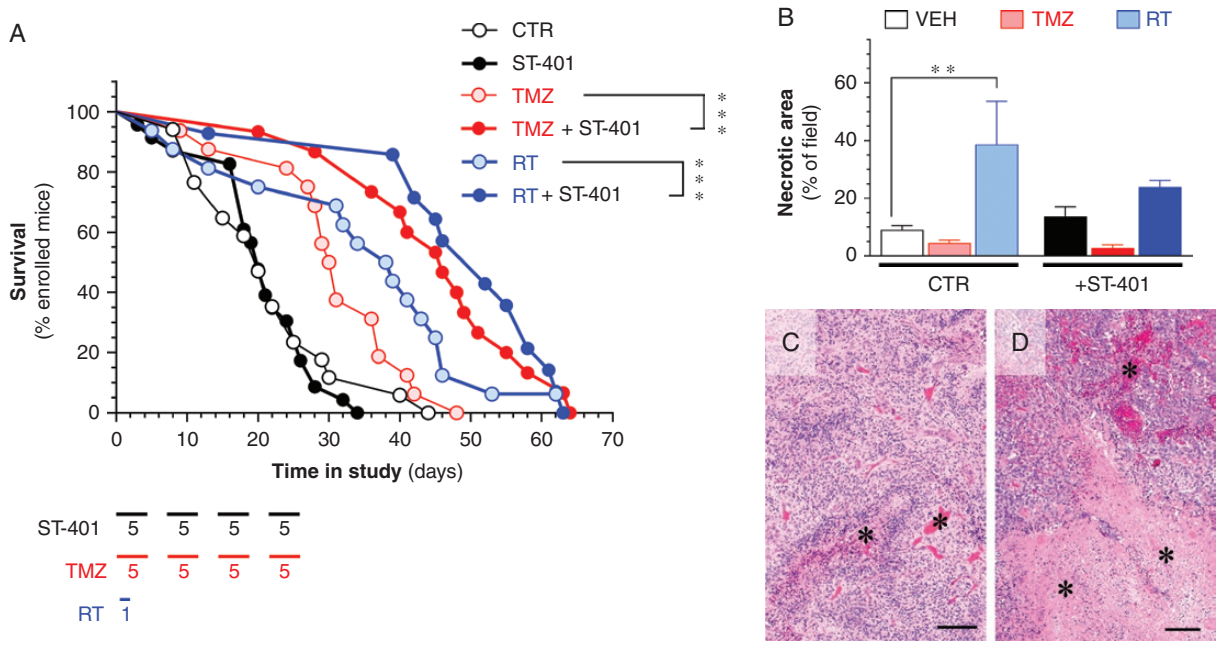

Figure 5. ST-401 enhances the therapeutic efficacy of RT and TMZ in a PDGFB-glioma mouse model. (A) Survival of PDGFB-glioma mice treated with vehicle control (CTR, formulation only, white symbol), ST-401 (bidaily, 5 days/week for 4 weeks, black symbol), TMZ (50 mg/kg, once per day, 5 days/week for 4 weeks, light red symbol), TMZ + ST-401 (dark red symbol), RT (10-Gy, once, light blue symbol) and RT+ST-401 (dark blue symbol). Results are mean ± MEM of 10 mice per arm. Mantel Cox Test analysis indicated signifant difference of ***$P < .001$. (B–D) RT increases necrotic area in PDGFB-glioma as determined by histopathological analysis (B). Representative H&E stained sections of PDGFB-glioma in the CTR arm (C) and from the RT arm (D) illustrating the increase in necrotic area (asterixis) in the latter. Scale bar = 100 μm.

cancer cells and impaired cell migration, the combination of which reduce tumor mass and curbs malignancy.[30,31] Combined, these results showed that ST-401 treatment impacts PDGFB-glioma tumorigenesis by disrupting cell mitosis and morphology that results in increased tumor density, all of which is consistent with the MOA of MTAs.

Discussion

The highly invasive nature of glioma exemplifies the challenge of overcoming the BBB and achieving adequate drug delivery to residual, sometimes extensive, tumor remaining after resection as evidenced by the presence of infiltrating single glioma cells throughout brain parenchyma.[32] We report the development of a new chemical entity, the brain-penetrant MTA, ST-401, that disrupts multiple hallmarks of glioma tumorigenesis at nanomolar concentrations. ST-401 readily reached the brain of healthy mice (with intact BBB), a feature likely dues to its physicochemical properties and the absence of an efflux mechanism for this compound, thus resulting in brain micromolar concentrations that are above its antitumor EC_{50}s. Of note, ST-401 triggers a milder, yet rapid onset and fully reversible reduction in MT assembly, a response that has a more gentle effect on MT function than Noco. Noco was not clinically pursued because of its high toxicity in hematopoietic tissues.[21] The more gentle effect of ST-401 on MT dynamics suggests a promising safety profile for this new MTA.

Until recently, MTAs were thought to preferentially kill cancer cells because of their high proliferation rate, but we now know that the proliferation rate of many MTA-sensitive cancers is low and that tumor regression occurs only when the cytocidal effects of MTAs is not limited to dividing cells.[1,6] We show that ST-401 kills MGG8 cells in interphase. The dynamic behavior of the MT network in glioma in interphase represents an excellent target for MTA because its disruption will affect the trafficking of multiple factors, including DNA damage response proteins required during S phase.[30,33] The enhanced sensitivity of MGG8 cells in interphase to MTA as compared to T98G cells in interphase could be due to multiple reasons, including differences in mutations that alter interphase MT function and disruption of reliable trafficking of S phase factors.[4] ST-401 killed PD-glioma cells independent of their transcriptional subtype. This broad spectrum of antitumor activity addresses a key limitation of therapeutics that target oncoproteins and tumor suppressers and do not treat the heterogeneous nature glioma. We show that ST-401 inhibits the formation of TM that interconnect PD-glioma, providing the first evidence that: (1) TM networks can be inhibited pharmacologically, (2) proper MT function is necessary to establish this syncytium, and (3) TM of some PD-glioma cells (here S24) are particularly vulnerable to MTAs.[7] The differential response of S24 and BG5 might reflect their ability to form TMs. In general, S24 forms longer TMs compared to BG5 (TM length/cell: S24 = 310 μm and BG5 = 278 μm) with

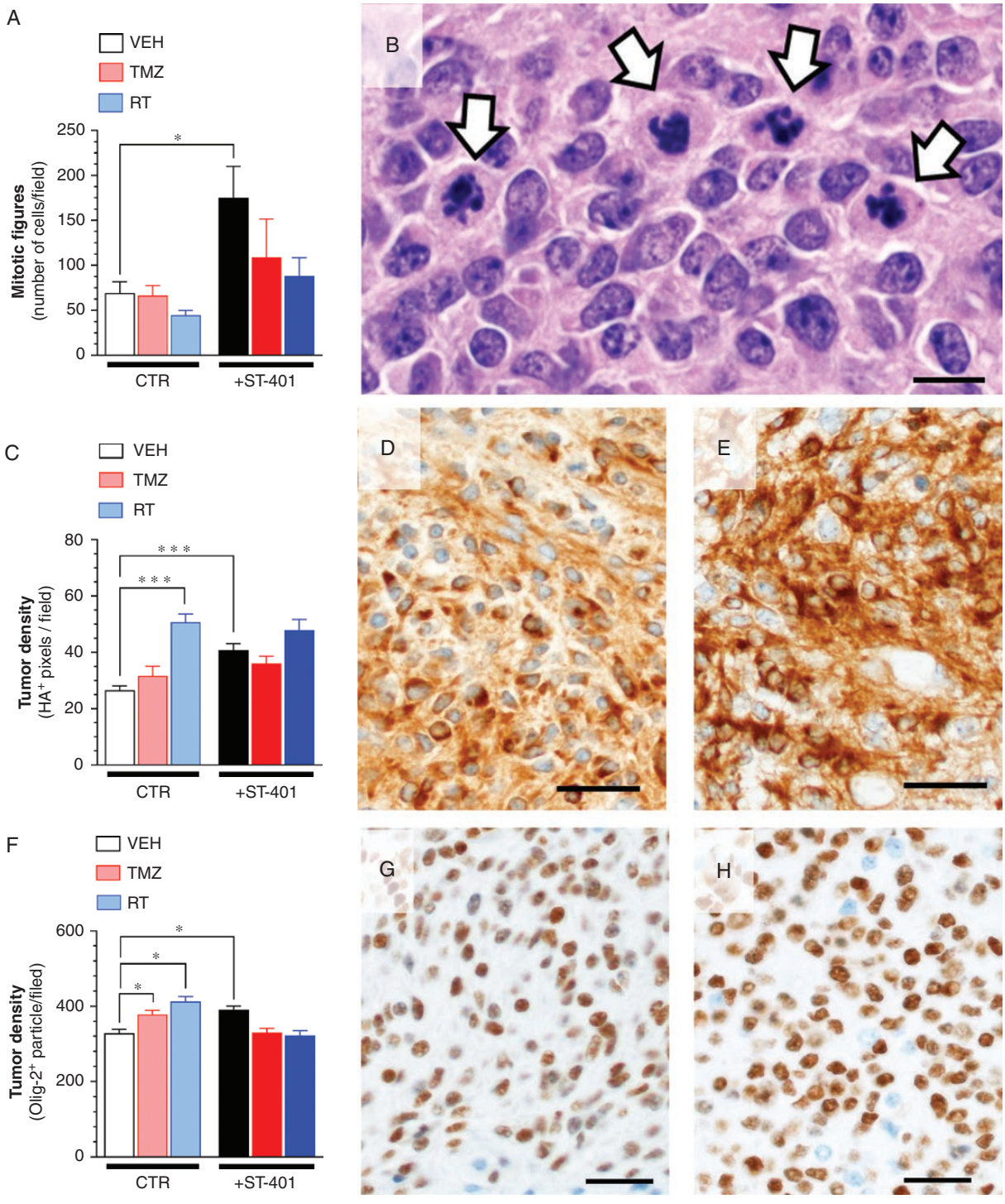

Figure 6. ST-401 disrupts mitosis and enhances PDGFB-glioma tumor density. (A) ST-401 increases the number mitotic figures in PDGFB-glioma as determined by H&E histopathological analysis. (B) Representative H&E stained section of PDGFB-glioma treated with ST-401 illustrating disrupted mitotic figures (arrows). Scale bar = 100 μm. (C) RT and ST-401 increase PDGFB-glioma tumor density as determined by HA imnumostaining. (D–E) Representative HA immunostaining of PDGFB-glioma from CTR (D) and ST-401 arms (E). Scale bars = 20 μm. (F) TMZ, RT and ST-401 increase PDGFB-glioma tumor density as determined by olig-2 imnumostaining. (G–H) Representative olig-2 immunostaining of PDGFB-glioma from CTR (G) and ST-401 arms (H). Tumor density (ie, % area) of positively-stained pixels counted by unbiased semi-quantitative analysis using Image J. Results are mean ± SEM from $n = 5–8$ brain sections per arm. Two-way ANOVA analysis followed by Tuckey's post-test indicated significant difference of $^{***}P < .001$, $^{**}P < .01$ and $^{*}P < .05$.

similar numbers of TMs per cell indicating longer TMs in S24 might be more susceptible to MTAs because they depend more on functional MT for stabilization. The vulnerability of PD-glioma cells in interphase and of PD-glioma TMs to brain-penetrant MTAs suggest developing treatments for glioma that combine brain-penetrant MTAs and DNA-damaging therapies to both kill malignant cells in interphase that compose most of the tumor burden, and disrupt their resistance-generating TM networks.

The lack of ST-401 single agent activity in the PDGFB-glioma model might be due to several reasons, including the presence of a native brain microenvironment that recapiluates glioma–stroma interactions occurring behind the BBB in the PDGFB-glioma model, and its single driving mutation (increased PDGFB activity) versus the mutations in PD-glioma isolates and their growing in culture. We show that a combination of ST-401 with TMZ and RT nearly doubled median survival in the PDGFB-glioma model, which represents one of the most pronounced therapeutic response measured in the model system, and provides an insight under what situation ST-401 might be useful in the clinic. Thus, ST-401 is a radiosensitizer that could increase the therapeutic efficacy of DNA-damaging treatments most likely by disruption interphase MT network and delaying DNA repair, and by disrupting TMs that traffick DNA damage response proteins between glioma cells.[30,33] In fact, the response of PDGFB-GBM to ST-401 more closely resemble S24/BG5 results in vitro, where the cytotoxic effects were attenuated as well. Both models are thought to form networks (although not formally shown for PDGFB-GBM), whereas most PD-GBM isolates in culture will not typically contain TM-connected cells. Another possible mechanism for the radiosensitizing mechanism is that the combination of ST-401, TMZ or RT might affects BBB functions and allows enhanced penetration of brain parenchyma.

An increase of the cellular density in highly diffuse PDGFB-glioma in response to ST-401 suggests impaired mitosis, cytotoxicity and anti-migratory effects, the combination of which curbs tumorigenesis. An effective anti-invasive therapy would certainly confer beneficial effects, as diffuse brain colonization hinders antitumor therapies, and single-infiltrated tumor cells might lead to dysfunction in areas distant from the tumor bulk. Anti-migratory effect of ST-401 would also inhibit the malignant repair response that follows surgeries, which is of potential clinical relevance since currently there are no such therapies available.[10,34,35] As such, MT function play a central role in glioma migration and their dismantling by MTA that disrupt the cell migration machinery, cell morphology, and overall dynamics of growing tumors has emerged as a promising therapeutic approach for the treatment of glioma.[31]

In summary, our study identifies novel traits of glioma tumorigenesis that exhibit enhanced sensitivity to MTAs, provides new rationals to develop brain-penetrant MTAs and describes ST-401 as a promising chemical scaffold to develop such neuro-oncology therapeutics. Brain-penetrant MTAs hold breakthrough potential as they harbor preclinical characteristics that promise therapeutic benefit for the treatment of patients diagnosed with glioma.

Supplementary Data

Supplementary data are available at *Neuro-Oncology Advances* online.

Keywords

DNA-damage | interphase | microtubules | tumor microtubes

Acknowledgments

Disclaimer. This research was supported in part by the Developmental Therapeutics Program in the Division of Cancer Treatment and Diagnosis of the National Cancer Institute, which includes federal funds under Contract No. HHSN261200800001E. The content of this publication does not necessarily reflect the views or policies of the Department of Health and Human Services, nor does mention of trade names, commercial products, or organizations imply endorsement by the U.S. Government.

Funding

This work was supported by the National Institutes of Health [P20GM103546, P30NS055022 to P.D. and R.R.P.] [R41NS105304, R43AR076842 to P.D. and N.B.W.] [R43CA165452 to E.C.H.] [R21NS106924, R01CA244213 to N.S. and L.W.] [R01GM069429 to M.W. and L.W.] and the German Research Foundation [SFB 1389 to F.W., E.J., and D.D.A.].

Conflict of interest statement. N.S. is professor at the University of Washington Seattle, founder of Stella Therapeutics, Inc. and employed by Stella Consulting LLC. The terms of this arrangement have been reviewed and approved by the University of Washington Seattle in accordance with its policies governing outside work and financial conflicts of interest in research. E.H., J.J. V., P.J. C., E.J., C.X., P.D., E.H., D.K.K., M.W., N.B., D.D.A., L.G.W, F.W., and E.C.H. declare no conflict of interest.

Authorship Statement. E.H., P.D., P.J. C., E.J., C.X., E.H., D.K.K., M.W., N.B., and D.D.A.: Performed experiments and wrote the manuscript. L.G.W.: Designed experiments, performed experiments and wrote the manuscript. F.W., E.C.H., and N.S.: Designed experiments and wrote the manuscript.

References

1. Mitchison TJ. The proliferation rate paradox in antimitotic chemotherapy. *Mol Biol Cell.* 2012;23(1):1–6.
2. Brouhard GJ, Rice LM. Microtubule dynamics: an interplay of biochemistry and mechanics. *Nat Rev Mol Cell Biol.* 2018;19:451–463.
3. Field JJ, Kanakkanthara A, Miller JH. Microtubule-targeting agents are clinically successful due to both mitotic and interphase impairment of microtubule function. *Bioorg Med Chem.* 2014;22(18):5050–5059.
4. Calinescu AA, Castro MG. Microtubule targeting agents in glioma. *Transl Cancer Res.* 2016;5(Suppl 1):S54–S60.
5. Herman JA, Toledo CM, Olson JM, DeLuca JG, Paddison PJ. Molecular pathways: regulation and targeting of kinetochore-microtubule attachment in cancer. *Clin Cancer Res.* 2015;21(2):233–239.
6. Abbassi RH, Recasens A, Indurthi DC, et al. Lower tubulin expression in glioblastoma stem cells attenuates efficacy of microtubule-targeting agents. *ACS Pharmacol Transl Sci.* 2019;2(6):402–413.
7. Osswald M, Jung E, Sahm F, et al. Brain tumour cells interconnect to a functional and resistant network. *Nature.* 2015;528(7580):93–98.
8. Linkous A, Balamatsias D, Snuderl M, et al. Modeling patient-derived glioblastoma with cerebral organoids. *Cell Rep.* 2019;26(12):3203–3211.e3205.
9. Weil S, Osswald M, Solecki G, et al. Tumor microtubes convey resistance to surgical lesions and chemotherapy in gliomas. *Neuro Oncol.* 2017;19(10):1316–1326.
10. Jung E, Alfonso J, Osswald M, Monyer H, Wick W, Winkler F. Emerging intersections between neuroscience and glioma biology. *Nat Neurosci.* 2019;22(12):1–10.
11. Oehler C, Frei K, Rushing EJ, et al. Patupilone (epothilone B) for recurrent glioblastoma: clinical outcome and translational analysis of a single-institution phase I/II trial. *Oncology.* 2012;83(1):1–9.
12. Steinmetz MO, Prota AE. Microtubule-targeting agents: strategies to hijack the cytoskeleton. *Trends Cell Biol.* 2018;28(10):776–792.
13. Diaz P, Horne E, Xu C, et al. Modified carbazoles destabilize microtubules and kill glioblastoma multiform cells. *Eur J Med Chem.* 2018;159:74–89.
14. Cherry AE, Haas BR, Naydenov AV, et al. ST-11: a new brain-penetrant microtubule-destabilizing agent with therapeutic potential for glioblastoma multiforme. *Mol Cancer Ther.* 2016;15(9):2018–2029.
15. Holland EC, Hively WP, DePinho RA, Varmus HE. A constitutively active epidermal growth factor receptor cooperates with disruption of G1 cell-cycle arrest pathways to induce glioma-like lesions in mice. *Genes Dev.* 1998;12(23):3675–3685.
16. Jaqaman K, Loerke D, Mettlen M, et al. Robust single-particle tracking in live-cell time-lapse sequences. *Nat Methods.* 2008;5(8):695–702.
17. Jung E, Osswald M, Blaes J, et al. Tweety-homolog 1 drives brain colonization of gliomas. *J Neurosci.* 2017;37(29):6837–6850.
18. Cimino PJ, Kim Y, Wu HJ, et al. Increased HOXA5 expression provides a selective advantage for gain of whole chromosome 7 in IDH wild-type glioblastoma. *Genes Dev.* 2018;32(7-8):512–523.
19. Ertych N, Stolz A, Stenzinger A, et al. Increased microtubule assembly rates influence chromosomal instability in colorectal cancer cells. *Nat Cell Biol.* 2014;16(8):779–791.
20. Jordan MA, Thrower D, Wilson L. Effects of vinblastine, podophyllotoxin and nocodazole on mitotic spindles. Implications for the role of microtubule dynamics in mitosis. *J Cell Sci.* 1992;102 (Pt 3):401–416.
21. Attia SM. Molecular cytogenetic evaluation of the mechanism of genotoxic potential of amsacrine and nocodazole in mouse bone marrow cells. *J Appl Toxicol.* 2013;33(6):426–433.
22. Brennan CW, Verhaak RG, McKenna A, et al.; TCGA Research Network. The somatic genomic landscape of glioblastoma. *Cell.* 2013;155(2):462–477.
23. Wakimoto H, Mohapatra G, Kanai R, et al. Maintenance of primary tumor phenotype and genotype in glioblastoma stem cells. *Neuro Oncol.* 2012;14(2):132–144.
24. Tannous BA, Kerami M, Van der Stoop PM, et al. Effects of the selective MPS1 inhibitor MPS1-IN-3 on glioblastoma sensitivity to antimitotic drugs. *J Natl Cancer Inst.* 2013;105(17):1322–1331.
25. Berg S, Kutra D, Kroeger T, et al. ilastik: interactive machine learning for (bio) image analysis. *Nat Methods.* 2019;16(12):1–7.
26. Oberoi RK, Parrish KE, Sio TT, Mittapalli RK, Elmquist WF, Sarkaria JN. Strategies to improve delivery of anticancer drugs across the blood-brain barrier to treat glioblastoma. *Neuro Oncol.* 2016;18(1):27–36.
27. Ene CI, Kreuser SA, Jung M, et al. Anti-PD-L1 antibody direct activation of macrophages contributes to a radiation-induced abscopal response in glioblastoma. *Neuro Oncol.* 2019;22(5):639–651.
28. Leder K, Pitter K, LaPlant Q, et al. Mathematical modeling of PDGF-driven glioblastoma reveals optimized radiation dosing schedules. *Cell.* 2014;156(3):603–616.
29. Hambardzumyan D, Becher OJ, Rosenblum MK, Pandolfi PP, Manova-Todorova K, Holland EC. PI3K pathway regulates survival of cancer stem cells residing in the perivascular niche following radiation in medulloblastoma in vivo. *Genes Dev.* 2008;22(4):436–448.
30. Markowitz D, Ha G, Ruggieri R, Symons M. Microtubule-targeting agents can sensitize cancer cells to ionizing radiation by an interphase-based mechanism. *Onco Targets Ther.* 2017;10:5633–5642.
31. Jamous S, Comba A, Lowenstein PR, Motsch S. Self-organization in brain tumors: how cell morphology and cell density influence glioma pattern formation. *PLoS Comput Biol.* 2020;16(5):e1007611.
32. Lemée JM, Clavreul A, Menei P. Intratumoral heterogeneity in glioblastoma: don't forget the peritumoral brain zone. *Neuro Oncol.* 2015;17(10):1322–1332.
33. Komlodi-Pasztor E, Sackett D, Wilkerson J, Fojo T. Mitosis is not a key target of microtubule agents in patient tumors. *Nat Rev Clin Oncol.* 2011;8(4):244–250.
34. Comba A, Dunn P, Argento AE, et al. 3131 oncostreams: novel dynamics pathological multicellular structures involved in glioblatoma growth and invasion. *J Clin Transl Sci.* 2019;3(s1):111.
35. Comba A, Zamler D, Argento AE, et al. CSIG-11. Oncostreams: novel structures that specify gliomas' self-organization, are anatomically discrete, functionally unique, and molecularly distinct. *Neuro Oncol.* 2017;19(Suppl 6):vi52.